ACS APPLIED MATERIALS & INTERFACES

LETTER

www.acsami.org

Stabilization of Embedded Pt Nanoparticles in the Novel Nanostructure Carbon Materials

Ping-Lin Kuo* and Chun-Han Hsu

Department of Chemistry and Chemical Engineering, National Cheng Kung University, Tainan, Taiwan 70101, ROC

Supporting Information

ABSTRACT: An extremely durable and highly active Pt catalyst has been successfully prepared by embedding Pt^0 nanoparticles inside the pores of the nitrogen-dotted porous carbon layer surrounding carbon nanotubes (Pt@NC−CNT). The Pt@NC−CNT catalyst has a high BET surface area of 271 $m^2\ g^{-1}$ (62 $m^2\ g^{-1}$ for Pt/XC-72) and comparably high electrochemically active surface area of 64.3 $m^2\ g^{-1}$ (68.2 $m^2\ g^{-1}$ for Pt/XC-72). The prepared Pt nanoparticles are small in size (2.8 ± 1.3 nm) and have a strong interaction of nitrogen to platinum, as evidenced by the binding energy observed at 399.5 eV. The maximum current densities (I_f) during methanol oxidation observed for Pt@NC−CNT (13.2 mA cm^{-1}) is 1.2 times higher than that of Pt/XC-72 (10.8 mA cm^{-1}) catalysts. Remarkably, in the long term durability test, the I_f after 1000 cycles for Pt@NC−CNT decreased to 10.6 mA cm^{-1} compared with Pt/XC-72, which decreased to 2.6 mA cm^{-2}. This means that the Pt@NC−CNT catalyst has a tremendously stable electrocatalytic activity for MOR because of the unique structure of Pt@NC−CNT formed in this novel synthesis technique.

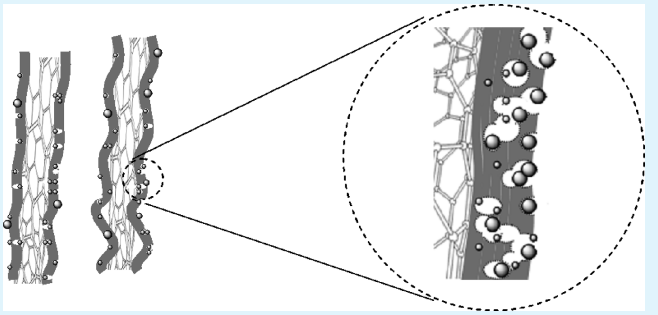

KEYWORDS: aniline, carbon nanotube, durability, methanol oxidation, porous carbon

A catalyst with high durability accompanied by high catalytic activity is a key issue for fuel cells and has attracted extensive attention.[1−5] Nitrogen-dotted carbon nanotubes (N-CNTs) reveal promising potential for DMFC catalyst application by means of affecting properties such as conductivity, nanostructure and catalyst activity.[6−8] Several methods for preparing N-CNT have been used, such as doping nitrogen directly during the synthesis of carbon materials or the post-treatment of presynthesized carbon materials with an N-containing precursor (N_2, NH_3, etc.).[6−15] Generally, Pt-based catalysts with nitrogen-containing carbon as support exhibit enhanced catalytic activity toward methanol oxidation and oxygen reduction,[16−18] which can be attributed to modifying the interaction between the Pt nanoparticles and carbon support.

In the present work, an extremely durable and highly active Pt catalyst was prepared by embedding Pt^0 nanoparticles inside the pores of the nitrogen dotted porous carbon layer surrounding carbon nanotubes (Pt@NC−CNT). In the preparation, aniline was used for three purposes: (1) to disperse the bundles of CNT into separated lines;[19] (2) to form polyaniline (PANI), which was then pyrolyzed into the N-dotted porous carbon layer surrounding CNT (NC−CNT); and (3) to stabilize Pt^{4+} and/or Pt^0 during the reduction and pyrolysis process.[19−21] Here, the dotted nitrogen found in the porous carbon layer not only acts as a stabilizer for preparing small Pt particles (2.8 ± 1.3 nm) but also enhances the catalytic activity as Pt is used to catalyze the oxidation. Meanwhile, Pt^0 particles inside NC−CNT are protected by being embedded inside the pores of nitrogen dotted carbon char, resulting in high durability. EDTA was used to chelate Pt^{4+} and Pt^0 in order to create a space between the Pt^0 and carbon char after the EDTA was pyrolyzed.

The Pt@NC−CNT was prepared as shown in Figure 1. First, aniline was used to efficiently separate the CNT bundles (Figure 1b) and then was mixed with the EDTA-chelated platinum-ions solution. Here, aniline adsorbs onto the surface of CNT to form aniline-stabilized CNT through the $\pi-\pi$ interaction between aniline and pristine CNT (Figure 1c).[19,22−24] After the polymerizing of aniline in situ (Figure 1d), a polyaniline (PANI) layer was coated onto the surface of the CNT and platinum ions were then wrapped inside the layer where EDTA chelates with Pt^{4+}. In the thermal cracking process, the PANI was cleaved to generate a porous nanostructure of nitrogen-containing carbon char as a shell surrounding the core of the CNT, meanwhile most of EDTA surrounding Pt^{4+} was pyrolyzed into gas to create the space between Pt and the char layer and enable a greater exposure of platinum, and the others (<10 wt %) formed carbon char.[25,26] After the reduction of platinum ion by $NaBH_4$, the novel Pt@NC−CNT catalyst was accomplished. For comparison purposes, we also synthesized a Pt@NC−CNT-x catalyst

Received: October 19, 2010
Accepted: December 21, 2010
Published: December 29, 2010

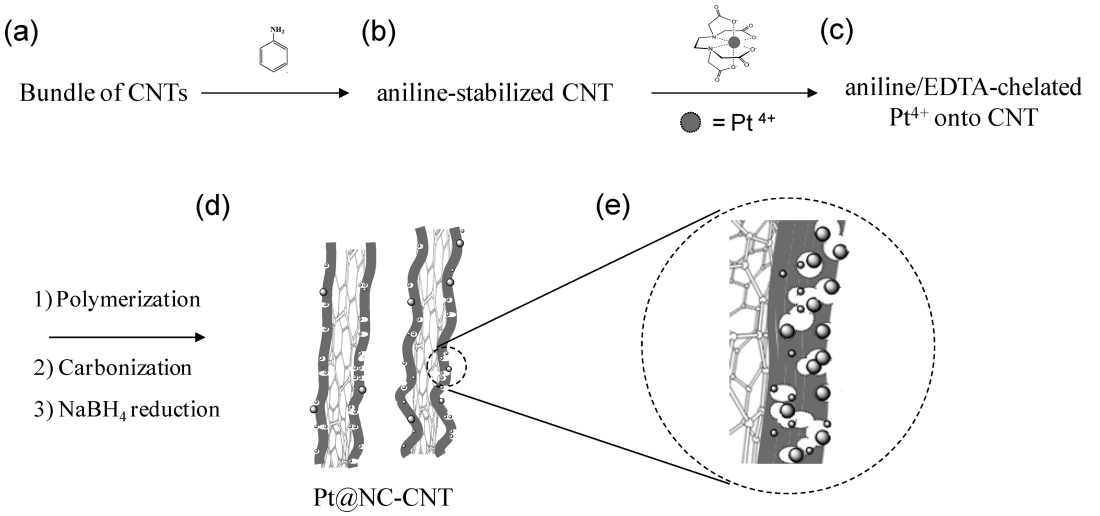

Figure 1. Synthetic procedure of Pt nanoparticles embedded in the pore of nitrogen-containing carbon layer on carbon nanotubes.

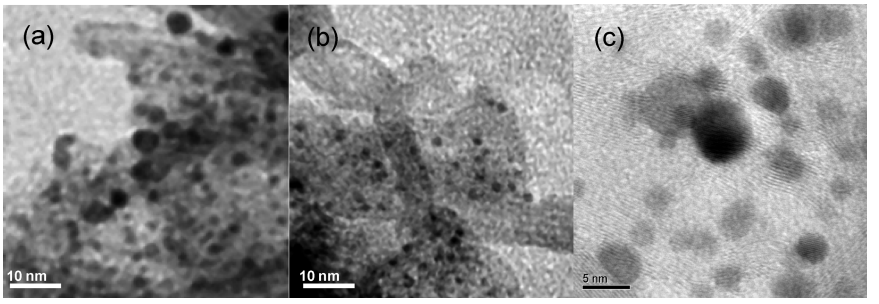

Figure 2. TEM images of (a) Pt@NC−CNT and (b) Pt@NC−CNT-x. HR-TEM image of (c) Pt@NC−CNT.

without using EDTA to chelate platinum ions, the results of which are presented below in the discussion section.

To further study the porosity of the carbon support, we measured the surface areas by N_2 adsorption/desorption. The results show that both Pt@NC−CNT (271 $m^2 g^{-1}$) and Pt@NC−CNT-x (120 $m^2 g^{-1}$) have a significantly higher BET surface area than that of Pt/XC-72 (62 $m^2 g^{-1}$). This indicates that the carbon char surrounding the CNT possesses high porosity inside the char and/or high roughness on the surface of the char because of the gases that occurred during the pyrolysis of PANI. For Pt@NC−CNT, the introduction of EDTA into PANI results in a 150% increasing in surface area. The higher surface area of carbon support not only increases depositing sites to help in dispersing and stabilizing the Pt nanoparticles but also enhances the diffusion of fuel during the reaction.[27−30] Here, the char linking of NC−CNT may act as a new conductive pathway to enhance the conductivity among the sidewalls of CNT.

The particle sizes and distribution of the Pt catalyst on different carbon supports were measured by TEM. Pt@NC−CNT (Figure 2a) and Pt@NC−CNT-x (Figure 2b) particles are all small (2.8 ± 1.3 and 1.6 ± 0.3 nm, respectively) and uniform. Figure 2c displays a typical high resolution TEM (HRTEM) image of the Pt@NC−CNT. The Pt nanoparticles are found to be surrounded by microporous graphite layers, which illustrates that the Pt nanoparticles are covered by a carbon layer. The Pt contents were quantified by thermogravimetric analysis (TGA) to be 20.4 and 12.9% for Pt@NC−CNT and Pt@NC−CNT-x, respectively (see Figure S1 in the Supporting Information). This means that the nitrogen species of polyaniline or dotted in the carbon layer can effectively stabilize Pt^{4+}/Pt^0, and favor the formation of small Pt nanoparticles.[16−18] The larger Pt nanoparticle size of Pt@NC−CNT indicates that the higher porosity induced by EDTA during the pyrolysis process, as measured by surface area, increases the aggregation of Pt^0 particles. The powder XRD patterns of Pt@NC−CNT and Pt@NC−CNT-x are shown in Figure S2 in the Supporting Information. The diffraction peaks in the XRD pattern at 2θ of 39.6, 46.1, 67.5, and 81.2° can be assigned to be the reflections of the (111), (200), (220), and (311) planes of the face-centered-cubic (fcc) Pt, respectively. The bandwidth became sharper for the Pt@NC−CNT catalyst, indicating an increase in particle size. The calculated grain sizes of these catalysts are in agreement with those determined by TEM.

The binding energy between Pt atoms and the nitrogen group on the surface of the NC−CNT was characterized by XPS as shown in Figure 3a. An observed peak is deconvoluted into five peaks centered at 398.5, 399.5, 400.8, 401.5, and 403 eV, which can be assigned to the pyridinic-type, nitrile, pyrrolic-type, graphitic-type, and oxidized nitrogen, respectively[16]. It is clear that Pt@NC−CNT contains large percentages of pyridinic and pyrrolic types of nitrogen, which are reported to be responsible for the active sites. Here, the strong interaction of nitrogen to platinum is evidenced by the clearly observed peak of nitrile. The nitrogen content in the char on the surface was measured by XPS, and showed that the N/C ratio was 7.2%, which is close to those obtained by EDS.

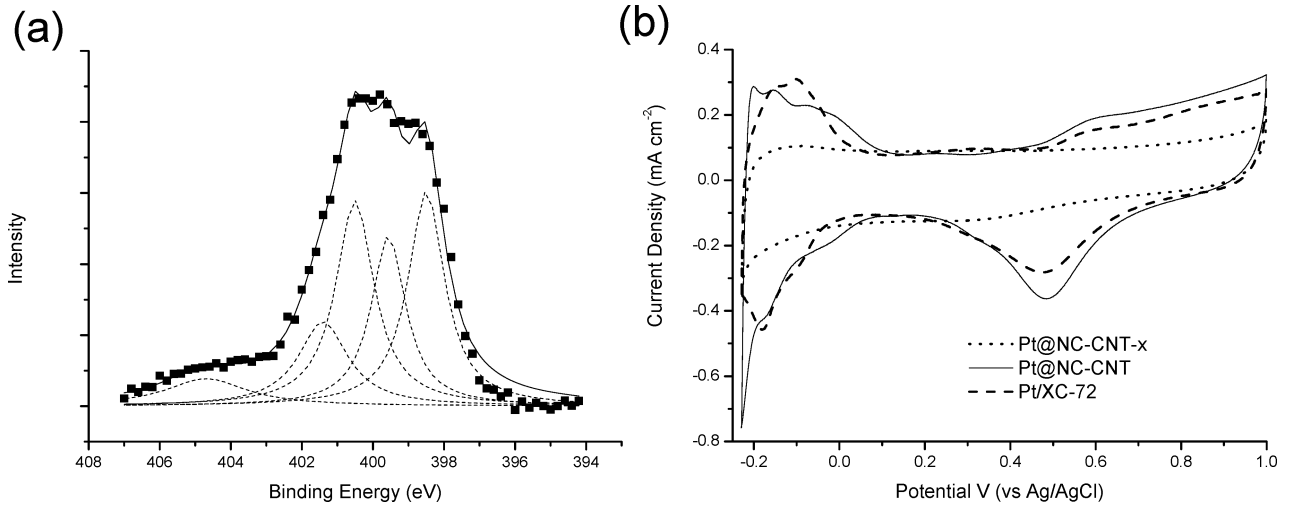

Figure 3. (a) XPS of N_{1s} of Pt@NC−CNT catalyst; (b) CV curves of Pt@NC−CNT-x, Pt@NC−CNT and Pt/XC-72 in 0.1 M $HClO_{4(aq)}$ at a scan rate of 20 mV s^{-1}.

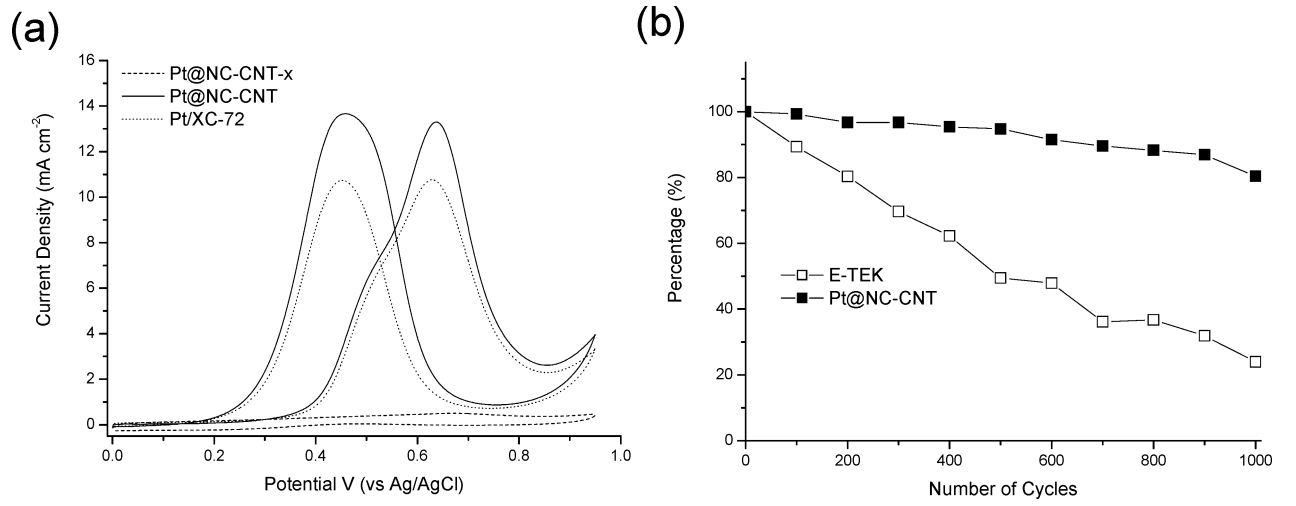

Figure 4. (a) CV curves of Pt@NC−CNT-x, Pt@NC−CNT, and Pt/XC-72; (b) loss of current density (I_f) of Pt/C catalyst with number of CV cycles in 1.0 M MeOH + 0.5 M $H_2SO_{4(aq)}$ at a scan rate of 20 mV s^{-1}.

To illustrate how the nitrogen-doped shell on the CNT affects the electrochemical properties of Pt embedded in NC−CNT, we measured the electrochemically active surface areas (EAS).[31−33] For the cyclic voltammograms (CV) of the Pt/C catalyst (Figure 3b), the EAS was 64.3 $m^2\ g^{-1}$ for Pt@NC−CNT and 1.3 $m^2\ g^{-1}$ for Pt@CNT-x. The lower EAS value of Pt@NC−CNT-x can probably be attributed to the carbon char wrap Pt catalyst. The higher EAS value of Pt@NC−CNT is probably induced by the Pt^0 particle surface being separated from the carbon char and becoming more exposed, which is caused by the adsorbed EDTA being pyrolyzed.

Voltammetric curves in N_2 saturated 0.5 M H_2SO_4 and 1.0 M MeOH aqueous solution are shown in Figure 4a.[34,35] The maximum current densities during methanol oxidation were measured from voltammetric curves for Pt@NC−CNT (13.2 mA cm^{-2}), Pt@NC−CNT-x (0.51 mA cm^{-2}) and Pt/XC-72 electrode (10.8 mA cm^{-2}). For Pt@NC−CNT-x, the low value in maximum current density (I_f) corresponds to its low EAS. It contrary to Pt@NC−CNT-x, Pt@NC−CNT showed a 25 times higher value than Pt@NC−CNT-x, and a 1.2 times higher value than Pt/XC-72 in catalytic activity because the surface of the Pt nanoparticles are exposed, which coincides with the results of the EAS. This further illuminates that the function of the EDTA used for preparing Pt@NC−CNT in this novel synthesis technique is of paramount importance to the catalytic ability of the methanol oxidation reaction (MOR).

The electrocatalyst durability of the Pt@NC−CNT and of Pt/XC-72 was evaluated through repeated CV cycles with the appropriate lower and upper potential limits in a 0.5 M H_2SO_4 and 1.0 M MeOH solution. The variation in the current density for MOR as a function of cycle number was 76 and 20% for Pt/XC-72 and Pt@NC−CNT, respectively (Figure 4b). This means that the Pt@NC−CNT catalyst has extremely stable electrocatalytic activity for MOR owing to the unique structure of Pt@NC−CNT, where Pt is protected by being embedded inside the porous N-doped carbon char.

In summary, a novel and highly durable Pt embedded nitrogen-containing carbon char layer on a carbon nanotube catalyst (Pt@NC−CNT) has been successfully prepared by using PANI as a source for both carbon and nitrogen. The Pt@NC−CNT catalyst possesses a high BET surface area (271 $m^2\ g^{-1}$)

(Pt/XC-72 catalyst, 62 $m^2\ g^{-1}$) and an EAS comparable (63.4 $m^2\ g^{-1}$) to the Pt/XC-72 catalyst (68.2 $m^2\ g^{-1}$). Furthermore, the I_f during methanol oxidation observed for Pt@NC−CNT is 1.2 times higher than Pt/XC-72 catalysts. In addition, Pt@NC−CNT offer extremely stable electrocatalytic activity, as is demonstrated by the variation in the I_f as a function of cycle number; for Pt/XC-72, it was 76% after 1000 cycles, while for the Pt@NC−CNT catalyst, it was 20% after 1000 cycles. The extremely stable electrocatalytic characteristic of the Pt@NC−CNT catalyst for MOR, observed from the variation in I_f, is due to the unique structure of Pt@NC−CNT formed in this novel synthesis technique.

■ ASSOCIATED CONTENT

Supporting Information. Experimental details (PDF). This material is available free of charge via the Internet at http://pubs.acs.org.

■ AUTHOR INFORMATION

Corresponding Author

*Tel.: 886-6-2757575-62658. Fax: 886-6-2762331. E-mail:plkuo@mail.ncku.edu.tw.

■ ACKNOWLEDGMENT

The authors thank the National Science Council, Taipei, ROC, for their generous financial support of this research.

■ REFERENCES

(1) Litster, S.; McLean, G. *J. Power Sources* **2004,** *130,* 61–76.
(2) Gupta, G.; Slanac, D. A.; Kumar, P.; Wiggings-Camacho, J. D.; Kim, J.; Ryoo, R.; Stevenson, K. J.; Johnston, K. P. *J. Phys. Chem. C* **2010,** *114,* 10796–10805.
(3) Choi, W.-C.; Woo, S.-I.; Jeon, M.-K.; Sohn, J.-M.; Kim, M.-R.; Jeon, H.-J. *Adv. Mater.* **2005,** *17,* 446–451.
(4) Wang, X.; Li, W.; Chen, Z.; Waje, M.; Yan, Y. *J. Power Sources* **2006,** *158,* 154–159.
(5) Liu, H.; Song, C.; Zhang, L.; Zhang, J.; Wang, H.; Wilkinson, D. P. *J. Power Sources* **2006,** *155,* 95–110.
(6) Shao, Y.; Sui, J.; Yin, G.; Gao, Y. *Appl. Catal., B* **2008,** *79,* 89–99.
(7) Gong, K.; Du, F.; Xia, Z.; Durstock, M.; Dai, L. *Science* **2009,** *323,* 760–764.
(8) Vijayaraghavan, G.; Stevenson, K. J. *Langumir* **2007,** *23,* 5279–5282.
(9) Matter, P. H.; Zhang, L.; Ozkan, U. S. *J. Catal.* **2006,** *239,* 83–96.
(10) Vinu, A.; Strinivasu, P.; Mori, T.; Sasaki, T.; Asthana, A.; Ariga, K.; Hishita, S. *Chem. Lett.* **2007,** *36,* 770–771.
(11) Trchova, M.; Konyushenko, E. N.; Stejskal, J.; Kovarova, J.; Ciric-Marjanovic, G. *Polym. Degrad. Stab.* **2009,** *94,* 929–938.
(12) Wu, G.; Li, D.; Dai, C.; Wang, D.; Li, N. *Langmuir* **2008,** *24,* 3566–3575.
(13) Wang, X.; Lee, J.-S.; Zhu, Q.; Liu, J.; Wang, Y.; Dai, S. *Chem. Mater.* **2010,** *22,* 2178–2180.
(14) Bezerra, C. W. B.; Zhang, L.; Lee, K.; Liu, H; Marques, A. L. B.; Marques, E. P.; Wang, H.; Zhang, J. *Electrochim. Acta* **2008,** *53,* 4937–4951.
(15) Lei, Z.; Zhao, M.; Dang, L.; An, L.; Lu, M.; Lo, A.-Y.; Yu, N.; Liu, S.-B. *J. Mater. Chem.* **2009,** *19,* 5985–5995.
(16) Niwa, H.; Horiba, K.; Harada, Y.; Oshima, M.; Ikeda, T.; Terakura, K.; Ozaki, J.-I.; Miyata, S. *J. Power Sources* **2009,** *187,* 93–97.
(17) Matter, P. H.; Wang, E.; Ozkan, U. S. *J. Catal.* **2006,** *243,* 395–403.
(18) Ikeda, T.; Boero, M.; Huang, S. F.; Terakura, K.; Oshima, M.; Ozaki, J. *J. Phys. Chem. C* **2008,** *112,* 14706–14709.
(19) Hsu, C. H.; Liao, H. Y.; Kuo, P. L. *J Phys. Chem. C* **2010,** *114,* 7933–7939.
(20) Chen, W. F.; Wang, P. J.; Hsu, C. H.; Jhan, J. Y.; Teng, H. S.; Kuo, P. L. *J Phys. Chem. C* **2010,** *114,* 6976–6982.
(21) Kuo, P. L.; Chen, W. F.; Lin, C. Y. *J. Power Sources* **2009,** *194,* 234–242.
(22) Mu, Y.; Liang, H.; Hu, J.; Liang, L.; Wan, L.; *J. Phys. Chem. B* 109 (**2005**) *109* 22212−22216.
(23) Hsin, Y. L.; Hwang, K. C.; Yeh, C. T. *J. Am. Chem. Soc.* **2007,** *129,* 9999–10010.
(24) Kin, K. K.; Yoon, S. M.; Choi, J. Y.; Lee, J.; Kim, B. K.; Kim, J. M.; Lee, J. H.; Paik, U.; Park, M. H.; Yang, C. W.; An, H.; Chung, Y.; Lee, Y. H. *Adv. Funct. Mater.* **2007,** *17,* 1775–1783.
(25) Wang, H. W.; Chung, M. R. *Mater. Chem. Phys.* **2003,** *77,* 853–859.
(26) Wang, H. W. *Mater. Chem. Phys.* **2002,** *74,* 1–4.
(27) Ambrosio, E. P.; Francia, C.; Gerbaldi, C.; Penazzi, N.; Spinelli, P.; Manzoli, M.; Ghiotti, G. *J. Appl. Electrochem.* **2008,** *38,* 1019–1027.
(28) Liu, S.-H.; Yu, W.-Y.; Chen, C.-H.; Lo, A.-Y.; Hwang, B.-J.; Chien, S.-H.; Liu, S.-B. *Chem. Mater.* **2008,** *20,* 1622–1628.
(29) Du, H.; Gan, L.; Li, B.; Wu, P.; Qiu, Y.; Kang, F.; Fu, R.; Zeng, Y. *J. Phys. Chem. C* **2007,** *111,* 2040–2043.
(30) Xu, W.; Zhou, X.; Liu, C.; Xing, W.; Lu, T. *Electrochem. Commun.* **2007,** *9,* 1002–1006.
(31) Han, S. B.; Song, Y. J.; Lee, J. M.; Kim, J. Y.; Park, K. W. *Electrochem. Commun.* **2008,** *10,* 10444–1047.
(32) Lim, B.; Jiang, M.; Camargo, P. H. C.; Cho, E. C.; Tao, J.; Lu, X.; Zhu, Y.; Xia, Y. *Science* **2009,** *324,* 1302–1305.
(33) Zhang, J.; Sasaki, K.; Sutter, E.; Adzic, R. R. *Science* **2007,** *315,* 220–222.
(34) Mu, Y.; Liang, H; Hu, J.; Jiang, L.; Wan, L. *J. Phys. Chem. B* **2005,** *109,* 22212–22216.
(35) Girishkumar, G.; Vinodgopal, K.; Kamat, P. V. *J. Phys. Chem. B* **2004,** *109,* 19960–19966.